RSC Advances

Journal Name

COMMUNICATION

A Facile Solvent-Free Route to Synthesize Ordered Mesoporous Carbons

Qiaowei Wang,[a,b] Yijie Mu[a], Weili Zhang[a], Liangshu Zhong[a], Yan Meng[a,*], Yuhan Sun[a,c,*]

**A novel solvent-free route is developed to synthesize a series of highly ordered mesoporous carbons (OMCs) and functionalized OMCs from solid raw materials. Compared with the widely used hydrothermal and EISA method, such route with avoidance of additional solvent for the preparation of OMCs is more convenient and efficient.**

Order mesoporous carbons (OMCs) have attracted much attention because of their unique properties and potential applications in diverse fields including energy, environment protection and catalysis[1-5] Various synthesis strategies such as nanocasting method with mesoporous silica as hard template[6,7]and organic-organic self-assembling method with amphiphilic surfactant or block copolymer as soft template,[8-12] have been widely adopted for preparation of order mesoporous carbons. Due to avoiding extra steps to prepare and thereafter sacrifice the ordered mesoporous silica, the organic-organic self-assembly method is much simple. However, for the self-assembly method, including both solvent evaporation induced self-assembly (EISA) and hydrothermal method, it normally takes a long time for the formation of mesostructured composite between carbon precursor and block copolymer separated from the diluted solution, which leads to lower efficiency and higher solvent waste.

Solvent-free route has long been applied to synthesis of many ceramic oxides, hydride, and nitride and is now being extended into a wide range of organic synthesis.[13,14] It has many advantages, such as reduced pollution, low cost, and simplicity in process and handling, which are especially important in industry. Considering these merits, recently, solvent-free route has been developed to prepare nanomaterials, such as zeolites, N, B-doped graphitic carbon, and carbon nanotube. Xiao et al. reported the solvent-free synthesis of various zeolites.[15,16] Obviously, it is very desirable to develop a solvent-free approaches to synthesis of OMCs .
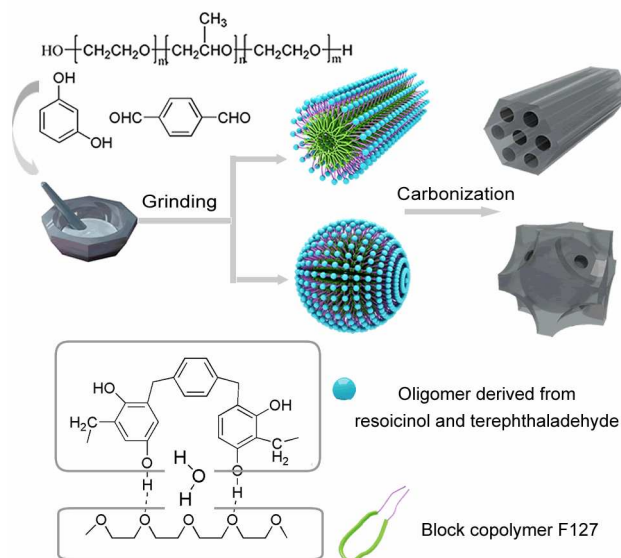
Scheme 1. Scheme for the solvent-free synthesis of OMCs.

Herein we present a facile and reproducible solvent-free synthesis route for OMCs by simply mixing, grinding, heating and carbonizing the carbon precursors with block copolymer (Scheme 1). Similar to the reported mesoporous carbon,10 the obtained mesostructures of carbon from solvent-free synthesis can be flexibly tuned from 2-D hexagonal (*p6m*) to 3-D caged cubic (*Im3m*) symmetry by varying the mass ratio of carbon precursors to the surfactant. Since no solvent is used, the space for solvent is saved and thus it is facile to prepare a large amount of mesoporous carbon in one-pot. Moreover, the solvent-free route can be applied to prepare functionalized OMCs by directly introducing the functional precursors during the grinding process.

Journal Name

COMMUNICATION

Table 1. Textural properties of H-OMC, C-OMC, N-OMC, Mo-OMC and F-OMC nanocomposites produced by solid-phase synthesis method

Sample	BET surface area[a] /m^2 g^{-1}	micropore area[b] /m^2 g^{-1}	pore volume[c] /cm^3 g^{-1}	pore size[d] /nm	unit cell parameter[e] /nm	wall thickness[f] /nm	content/wt%
H-OMC	700	380	0.55	5.4	11.8	6.4	-
C-OMC	420	170	0.26	4.4	14.9	8.5	-
N-OMC	390	290	0.26	4.2	10.3	6.1	17.0[g]
Mo-OMC	740	450	0.60	5.6	11.9	6.3	4.7[h]
F-OMC	790	400	0.72	6.7	12.9	6.2	-

[a] Calculated by the BJH model (Barret-Joyner-Halenda) from adsorption data in the range of P/P_0 0.05-0.20. [b] Calculated by the V-t method from adsorption branches of the N$_2$ isotherms in the range of P/P_0 0.30-0.50. [c] Estimated from the adsorbed amount of nitrogen at $P/P_0 > 0.995$. [d] Calculated by the BJH model from the adsorption branches of the isotherms. [e] Calculated from small angle XRD results using the Braggs diffraction formula of $2d\sin\theta = n\lambda$, and the unit cell parameters were calculated from the formula of $a = 2d_{100}/3^{1/2}$ for samples of 2-D hexagonal symmetry and $a = d_{110}*2^{1/2}$ for cubic carbon of C-OMC . [f] Calculated by the formula $h = a – D$ for 2-D hexagonal symmetry and $h = 0.5*3^{1/2}a - D$, where a represents the unit cell parameter and D represents the pore size diameter determined by the BJH model. [g] Nitrogen content determined by elemental analysis. [h] Mo$_2$C content calculated by XPS data.

Solvent-free synthesis of OMC is performed by mixing the solid raw materials of resorcinol, terephthalaldehyde, and block copolymer F127 (Supporting Information). After grinding for 5 min, a sticky paste-like mixture is obtained. Followed by heating and carbonizing the mixture, the OMCs (Table 1) with hexagonal (denoted as H-OMC) and cubic (denoted as C-OMC) structures are obtained (Table S1). The functionalized OMCs, N-doped OMC (denoted as N-OMC) and Mo$_2$C/OMC (denoted as Mo-OMC) nanocomposites are prepared with the same procedure by use of melamine and phosphomolybdic acid (PMA) as functional precursors.

The XRD pattern (Figure 1A-a) of H-OMC shows an intense diffraction peak and two weak peaks that can be indexed as 100, 200 and 210 reflections associated with 2-D hexagonal *p6m* symmetry. This observation indicates that H-OMC has a high degree of hexagonal mesoscopic organization as the previously reported OMC FDU-15.[17] The unit cell parameter calculated from the intense 100 peak was 11.8 nm. The SAXS pattern (Figure S1A) of as-made H_OMC shows an intense diffraction peak, indicating the ordered mesostructure formed after grinding and heating at 100°C. Heating this sample at600^{o}C under N$_2$ atmosphere gives a more resolved SAXS pattern. The lattice of the framework shringks by about 5.2 nm. TEM images of H-OMC (Figure 2a, b) show well-ordered stripe-like and hexagonally arranged mesopores, further confirming a high-quality hexagonal *p6m* mesostructure. N$_2$ sorption isotherms (Figure 1B-a) of H-OMC are typical type-Ⅳ curves with sharp capillary condensation step in the P/P_0 range of 0.40-0.70 and an H$_1$-type hysteresis loop, suggesting that H-OMC has uniform cylindrical mesoporous channels, similar to those of FDU-15. The BET surface area and the total pore volume of H-OMC are calculated to be 700 m^2 g^{-1} and 0.55 cm^3 g^{-1}, respectively. The pore diameter is about 5.4 nm (Figure S2), which is little bigger than that of FDU-15. This might be ascribed to the rigid frameworks formed by all-aromatic based substrates. The wall thickness is estimated to be 6.4 nm. Elemental analysis reveals that H-OMC consisits of C (80.8%), H (2.3 %), O (16.9 %) with C/H/O molar ratio of 1:0.33:0.16, suggesting a carbon framework. In addition, the 3D cubic C-OMC can be prepared with a low F127 content as in the case for FDU-16 via solvent-free synthesis.[17] The XRD patter of C-OMC (Figure 1A-b) shows four clear peaks that can be indexed as 110, 200, 211, and 310 of the body-centered
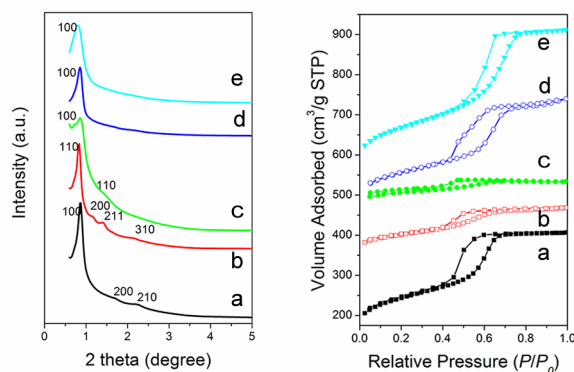

Figure 1. Small angle XRD patterns (A) and nitrogen sorption isotherms (B) of H-OMC (a), C-OMC (b), N-OMC (c), Mo-OMC (d), and F-OMC (e) prepared via solvent-free synthesis method. The isotherms of C-OMC, N-OMC, Mo-OMC and F-OMC are offset vertically by 300, 400, 350 and 450 cm^3/g, respectively.
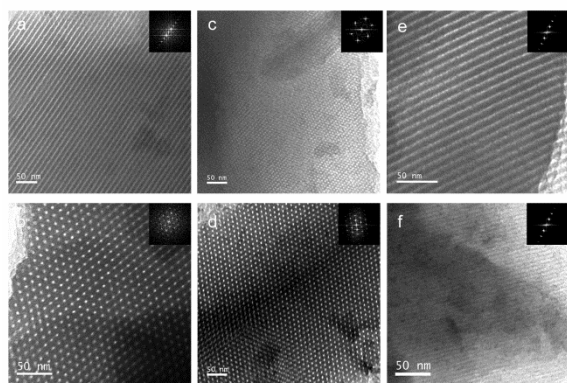
Figure 2. TEM images of H-OMC (a, b); C-OMC (c, d); N-OMC (e), and Mo-OMC (f) viewed along the [110] (a, c, e, f), [001] (b) and [111] (d) directions. The insets are the corresponding fast Fourier transform (FFT) diffractograms.

cubic space group ($Im3m$). As shown in SAXS patterns (Figure S1B), the ordered cubic mesostructure forms beform carbonization. The lattice shrinkage is about 4.6 nm (23.6%), which is slinghtly smaller than that for H-OMC (30.6%).The large domain regularity of C-OMC is further verified by TEM images (Figure 2c, d) viewed along the [110] and [111] directions, together with the corresponding fast Fourier transform (FFT) diffractograms (Figure 2c, d, inset). N_2 sorption isotherms (Figure 2B-b) of C-OMC show typical type-IV curves with an H_2-type hysteresis loop corresponding to a 3D caged pore structure. C-OMC has a BET surface area of 420 m^2 g^{-1}, a pore volume of 0.26 cm^3 g^{-1}, and a narrow pore size distribution at about 4.4 nm. Elemental analysis shows a composition of C-OMC with a molar ratio of C/H/O = 1:0.33:0.08 (C 88.0%, H 2.4%, O 9.6 %).

Thermogravimetric curves (Figure S3) show that significant weight losses occurred from 270 to 450 °C. This weight loss can be attributed to the decomposition of copolymer F127. The carbonization yield after calcined at 600 °C is 28 and 32 % for H-OMC and C-OMC, respectively. The Raman spectra of H-OMC (Figure S4) show a broad peak at 1317 cm^{-1} corresponding to the D band, and overlaps with the G band at 1562 cm^{-1}, indicative of a glassy carbon framework.

By addition of functional precursor during the grinding process, OMCs with various functionalized framework are successful prepared in one-pot, such as N-doped OMC (N-OMC) and Mo$_2$C/OMC nanocomposite (Mo-OMC). Figure 1c, d illustrate the XRD patterns of N-OMC and Mo-OMC. One intense diffraction peak can be seen on each sample, indicating the ordered hexagonal mesostructure remained after adding the functional precursors. For N-OMC, CHN analysis shows a high nitrogen content of 17 wt%. The nitrogen binding configurations in N-OMC were evaluated by XPS (Figure S5). Curve deconvolution shows that N$_{1s}$ spectra can be well-fitted to the superposition of four peaks, which can be assigned to pyridine- (N-6, 398.3 eV), pyrrole- or pyridine- (N-5, 400.0 eV), quaternary (N-Q, 401.2 eV) and oxidized like nitrogen species (402.8 eV), respectively. For Mo-OMC, intense diffraction peaks in the WXRD patterns (Figure S6) at 2θ of 34.3°, 39.3°, 61.6° and 74.8° are attributed to the structure of Mo$_2$C (PDF No. 35-0787), indicating the formation of well-crystallized Mo$_2$C. Figure 2e, f present the TEM images of N-OMC and Mo-OMC. In good agreement with XRD patters, the well-ordered mesostructures can be clearly observed on functionalized OMCs samples. As shown in the

TEM images of Mo-OMC, Mo$_2$C particles with sizes of ~3.5 nm are highly dispersed in the carbon framework.

Without addition of solvent, solvent-free synthesis increase the choices for functional precursor and decreases the influence on the self-assembly of carbon precursor and block copolymer. Thus, it is beneficial to introduce functional precursor to achieve high level functionlization. As far as N-doped OMC is concerned, melamine was well-known as nitrogen doping agent. However, it is hard to achieve high nitrogen doping due to poor solubility of melamine for conventional methods. In our work, as no solvent is used, high amount of melamine can be introduced while retain the ordered mesostructure, which yielded a remarkably high nitrogen doping content of 17.0 wt% based on elemental analysis. Such high nitrogen doping would be very attractive for many applications such as CO$_2$ adsorption and catalyst support. As for Mo$_2$C, Keggin acids are widely used as the precursors, in which Mo species is in anionic form.[18] The anion has strong interaction with block copolymer micelles in the solution and can perturb the long-range order of self-assembly.[19] However, the solvent-free route effectively decreases the interaction and leads to an ordered mesoporous Mo$_2$C/OMC nanocomposite with high Mo$_2$C loading amount of 4.7 wt% based on XPS results (Figure S7).

In conventional self-assembly method, the hydrogen bonding between hydrophilic blocks of F127 and carbon precursors acts as a driving force for the formation of the ordered mesostructures.[9,10] In our work, a trace amount of H$_2$O (theoretically 0.49 g H$_2$O per 1 g resorcinol for H-OMC) is generated from the solid raw materials. Although such amount of H$_2$O is not enough to dissolve F127, it may facilitate the formation of H-bond between carbon precursors and F127. Resorcinol and formalin (37 wt% formaldehyde in H$_2$O) are also employed as carbon precursor to prepare OMC without addition of extra solvent. It is interesting that hexagonal mesoporous carbon (denoted as F-OMC) can be obtained without adding any solvent (Figure 1A-e). The amount of H$_2$O in the whole reaction system of resorcinol/formalin is calculated to be 1.19 g per 1 g resorcinol. This suggests that the large amount of additional solvent may not be necessary for synthesizing OMCs. Moreover, "solvent-free" synthesis saves the space of solvents, thus, giving the higher yield in one-pot (Figure S8).

The mesophase transformation from 2-D hexagonal to 3-D cubic has been achieved by increase the amount of carbon precursors. Similar shift has been reported.[17] It is known the precursor favors incorporation with PEO blocks of the copolymer due to the strong interactions via H-bonds between carbon precursor and hydrophilic blocks. This leads to swelling of the hydrophilic volume, while the hydrophobic volume per block remains essentially constant. This asymmetry induces a curvature at the PEO/PPO interface, owing to the connectivity of PEO and PPO blocks, the constraint of constant density and the minimization of chain stretching. A low amount of carbon precursor yields a hexagonal mesostructure. As the amount of carbon precursor increases, it cannot support the interfacial curvature corresponding to the changes of hydrophilic /hydrophobic volume ratio. As a result, the mesostructure shifts to cubic Im3m structures.

In summary, a series of OMCs including H-OMC, C-OMC, N-OMC, Mo-OMC and F-OMC have been successfully prepared from solvent-free synthesis through mechanically mixing of raw materials in the absence of extra solvent. Compared with widely used EISA and hydrothermal route, the solvent-free synthesis is more convenient and efficient and has great potential in preparation of OMCs in large-scale in one-pot. These OMCs are expected to have great potential applications. For example, the Mo-OMCs could be

used as a stable catalyst for higher alcohol synthesis via syngas. The N-doped OMC may be an excellent CO_2 adsorbent with high adsorption capacity. Further work on application of such OMCs is ongoing in our group.

Notes and references

[a] CAS Key Laboratory of Low-Carbon Conversion Science and Engineering, Shanghai Advanced Research Institute, Chinese Academy of Sciences, Shanghai 201210, P. R. China. mengy@sari.ac.cn,

[b] University of Chinese Academy of Sciences, Beijing 100049, P. R. China

[c] Institute of Coal Chemistry, Chinese Academy of Sciences, Taiyuan 030001, P. R. China. sunyh@sari.ac.cn. Phone/Fax: 086-021-20325142

†

Electronic Supplementary Information (ESI) available: Experimental details for preparation of OMCs via solvent-free mechanical grinding, pore size distribution, WXRD of Mo-OMC, SXRD of F-OMC. See DOI: 10.1039/c000000x/

1 R. Ryoo, S. H. Joo, M. Kruk and M. Jaroniec, *Adv. Mater.,* 2001, **13**, 677.

2 A. H. Lu and F. Schüth, *Adv. Mater.,* 2006, **18**, 1793.

3 C. D. Liang, Z. J. Li and S. Dai, *Angew. Chem., Int. Ed.,* 2008, **47**, 3696.

4 Y. Wan, Y. F. Shi, and D. Y. Zhao, *Chem. Mater.,* 2008, **20.** 932.

5 T. Y.Ma, L. Liu and Z. Y. Yuan, *Chem. Soc. Rev.,* 2013, **42**, 3977.

6 S. Jun, S. H. Joo, R. Ryoo, M. Kruk, M. Jaroniec, Z. Liu, T. Ohsuna and O. Terasaki, *J. Am. Chem. Soc.,* 2000, **122**, 10712.

7 M. Kruk, M. Jaroniec, T. W.Kim and R. Ryoo, *Chem. Mater.,* 2003, **15**, 2815.

8 C. D.Liang, K. L. Hong, G. A. Guiochon, J. W. Mays and S. Dai, *Angew. Chem., Int. Ed.,* 2004, **43**, 5785.

9 C. D. Liang and S. Dai, *J. Am. Chem. Soc.,* 2006, **128**, 5316.

10 Y. Meng, D. Gu, F. Q. Zhang, Y. F Shi, H. F Yang, Z. Li, C. Z. Yu, B. Tu and D. Y. Zhao, *Angew. Chem., Int. Ed..* 2005, **44**, 7053.

11 F. Q. Zhang, Y. Meng, D. Gu, Y. Yan, C. Yu, B. Tu and D. Y.Zhao, *J. Am. Chem. Soc.,* 2005, **127**, 13508.

12 A. H. Lu, B. Spliethoff and F. Schüth, *Chem. Mater.,* 2008, **20**, 5314.

13 K. Tanaka and F. Toda, *Chem. Rev.,* 2000, **100**, 1025.

14 R. E. Morris and S. L. James, *Angew. Chem., Int. Ed.,* 2013, **52**, 2163.

15 L. Ren, Q. M. Wu, C. G. Yang, L. F. Zhu, C. J. Li, P. L. Zhang, H. Y. Zhang, X. J. Meng and F. S. Xiao, *J. Am. Chem. Soc.,* 2012, **134**, 15173.

16 Y. Y. Jin, S. Qi, G. D. Qi, C. G.Yang, J. Xu, F. Cheng, X. J. Meng, F. Deng and F. S. Xiao, *Angew. Chem., Int. Ed.,* 2013, **52**, 9172.

17 Y. Meng, D. Gu, F. Q. Zhang, Y. F. Shi, L. Cheng, D. Feng, Z. X.Wu, Z. X. Chen, Y. Wan, A. Stein and D. Y. Zhao, *Chem. Mater.,* 2006, **18**, 4447.

18 H. Wang, A. Q. Wang, X. D. Wang and T. Zhang, *Chem. Commun.,* 2008, **22**, 2565.

19 G. S. Armatas, G. Bilis and M. *J.* Louloudi, *Mater. Chem.,* 2011, **21**, 2997.